

Galvanotaxis of human granulocytes: electric field jump studies

K. Franke and H. Gruler

Abteilung für Biophysik, Universität Ulm, Oberer Eselsberg, D-7900 Ulm, Federal Republic of Germany

Received November 10, 1989/Accepted in revised form May 24, 1990

Abstract. The static and dynamic responses of human granulocytes to an electric field were investigated. The trajectories of the cells were determined from digitized pictures (phase contrast). The basic results are: (i) The track velocity is a constant as shown by means of the velocity autocorrelation function. (ii) The chemokinetic signal transduction/response mechanism is described in analogy to enzyme kinetics. The model predicts a single gaussian for the track velocity distribution density as measured. (iii) The mean drift velocity induced by an electric field, is the product of the mean track velocity and the polar order parameter. (iv) The galvanotactic dose-response curve was determined and described by using a generating function. This function is linear in E for $E < E_0 = 0.78 \text{ V/mm}$ with a galvanotaxis coefficient K_G of $(-0.22 \text{ V/mm})^{-1}$ at 2.5 mM Ca^{++} . For $E > E_0$ the galvanotactic response is diminished. This inhibition is described by a second term in the generating function $(-K_G \cdot K_I(E - E_0))$ with an inhibition coefficient K_I of 3.5 (v) The characteristic time involved in directed movement is a function of the applied electric field strength: about 30 s at low field strengths and below 10 s at high field strengths. The characteristic time is 32.4 s if the cells have to make a large change in direction of movement even at large field strength (E-jump). (vi) The lag-time between signal recognition and cellular response was 8.3 s. (vii) The galvanotactic response is Ca^{++} dependent. The granulocytes move towards the anode at 2.5 mM Ca^{++} towards the cathode at 0.1 mM Ca^{++} . (viii) The directed movement of granulocytes can be described by a proportional-integral controller.

Key words: Chemokinesis – Galvanotaxis – Dose-response curve – E-jump – Granulocytes

I. Introduction

Polymorphonuclear leukocytes (= granulocytes) are attracted by sites of inflammation to combat invading microorganisms. There must exist some mechanism to account for the fact that these cells move toward, and then remain in the vicinity of sites of infection. The direction-determining mechanism(s) involved must be a function of some information transmitted to the leukocytes by the infected cells.

In the case of a chemical signal the directed locomotion is chemotaxis, while it is galvanotaxis in the case of an electrical signal. Gerish and Keller (1981) investigated the chemokinetic relaxation (or adaptation) behaviour by changing the concentration gradient of chemotactic molecules by means of two microelectrodes exposed very close to a migrating cell (concentration jump experiment). The disadvantage of that type of experiment was: (i) it is based on diffusing molecules and diffusion takes time (seconds to minutes) and (ii) in every experiment only one cell can be observed, so that many experiments have to be performed. One basic result was that granulocytes cannot react immediately to the exposed signal.

The relaxation (or adaptation) of granulocytes can also be investigated by necrotaxis, e.g. a red blood cell is lysed by a laser beam. Granulocytes do not react immediately to the altered environment. A minimal time-lag of about 10 s was observed (Gruler 1984). The merit of the necrotaxis experiment is that several cells in the viewing field can be observed. The disadvantage is that nothing is known about the necrotactic gradient.

The relaxation (or adaptation) of granulocytes can also be investigated by means of an electric field (E-jump) (Fukushima et al. 1954). An applied electric field builds up very fast (far less than a second) and at the same time all the cells in the viewing field can be investigated. Unfortunately the whole signal chain of the cell is not employed. Rapp et al. (1988) showed, that the essential protein in galvanotaxis is the G-protein which is next to the chemotactic receptor in the signal chain (Becker et al. 1987). Fukushima et al. (1954) published trajectories of

* Offprint requests to: H. Gruler

E-jump experiments: There exists a time-lag of 10 to 20 s between the application of the signal and the reaction of the cell. We will show that the lag-time and characteristic time of the adaptation or relaxation process are 8.3 and 32.3 s, respectively.

The directed movement of a cell in an electric field or in a concentration gradient is not perfect (the cells do not follow exactly the field lines). This indicates (i) that the automatic control unit of the cell for the directed movement is not optimized to a constant field and (ii) that two types of signal are involved in the signal transduction/response mechanism. A deterministic signal which originates from the applied vector field and a stochastic signal which originates from the noise source in the signal transduction system. It is expected, that the noise source is at the very beginning of the signal transduction system. The receptor binding fluctuation as noise source in the signal chain of chemotaxis and chemokinesis has been discussed (Tranquillo and Lauffenburger 1987; Tranquillo et al. 1988a). Here we show that for chemokinesis this concept cannot be correct.

A variety of cells including granulocytes, macrophages, fibroblasts, amoebae, slime molds, etc. have the ability to direct their movement in an electric field. Some cell types like granulocytes, monocytes, etc. migrate towards the anode and other cell types such as fibroblasts, neural crest cells, growth cones of neurones, grow toward the cathode (Erickson and Nuccitelli 1984). Some cells have the ability to move to the positive pole and other cell types to the negative pole. This picture is disturbed by the observations of Van Laere (1988) and Fukushima et al. (1953). Van Laere (1988) investigated the growth of hyphal tips and germ tubes of *Phycomyces blakesleeanus* and found that the cells grow towards the positive pole at low field strength and towards the negative pole at high field strength. McGillivray and Gow (1986) and Gruler and Gow (1990) showed for growing hyphal tips and germ tubes of *Neurospora crassa* that the response is linear in the electric field for small tube lengths. This linear response is explained by the field induced distribution of membrane-bound proteins essential for galvanotropism. For large tube length and large electric field strength, the galvanotropism is inhibited in *Neurospora crassa*. The inhibition is explained by the field induced change in the transmembrane potential difference. Here we will show, that the galvanotaxis of granulocytes also exhibits two effects – a linear response and a field-dependent inhibition – in analogy to the galvanotropism of growing cells.

Fukushima et al. (1953) observed that granulocytes move towards the anode at high pH and towards the cathode at low pH. Obviously the cellular environment can alter the type of the cellular response. This change in directional response of granulocytes as a function of proton concentration can be explained by the isoelectric point of an essential protein (G-protein) in the signal transduction chain as Rapp et al. (1988) have shown. Here we will show that the Ca^{++} concentration can also change the response of granulocytes. At high concentration, the cells move towards the anode but at low concentration towards the cathode.

II. Material and methods

1. Granulocytes

Granulocytes were separated from heparinized venous blood of healthy human blood donors on a Histopaque density gradient: Equal volumes of blood and of Hanks Balanced Salt Solution (HBSS) were mixed. The centrifuge tube contained layers of 3 ml Histopaque-1119, 3 ml Histopaque-1077, and 6 ml blood-HBSS solution. The cells were centrifuged for 20 min at 300 *g*. The granulocytes were found enriched between the two Histopaque regions. This layer was washed 3 times in plasma-HBSS of the same donor (first wash: 300 *g* for 10 min, second and third wash: 200 *g* for 10 min). In the experiments with controlled Ca^{++} concentrations, the concentration was measured with a Ca^{++} sensitive electrode, HBSS is exchanged by HBSS modified, which contained 0.1 mM Ca^{++} and Mg^{++} ions adjusted to 1 mM. The last wash was made with the same medium as in the experiment. All solutions were adjusted to pH 7.4 (stabilization with sodiumhydrogencarbonate (0.35 g/l) and 28 mM HEPES (N-2-hydroxyethylpiperazine-N'-2-ethanesulfonic acid). The cells were kept as long as possible in the plasma-HBSS. The air in all test tubes was enriched with CO_2 before they were closed.

2. Galvanotaxis chamber

An electric field is created in a galvanotaxis chamber by the electric current driven through the aqueous solution (medium). We used a galvanotaxis chamber similar to the one described previously (Rapp et al. 1988).

A drop of the cell suspension ($4 \cdot 10^6$ cells/ml) is transferred to a glass slide and then covered with a coverslip ($20 \cdot 30 \text{ mm}^2$). Capillarity makes a homogeneous thin film (10–30 μm). The long sides of the coverslip were attached with paraffin to the glass slide. On the small sides two assemblies consisting of two filter papers ($20 \cdot 20 \text{ mm}^2$), an enamel block ($20 \cdot 20 \cdot 0.5 \text{ mm}^3$) containing two parallel ribbons of metal (Ag) foil as power- ($7 \cdot 25 \text{ mm}^2$) and the measuring- ($4 \cdot 25 \text{ mm}^2$) electrode, were attached with paraffin to the glass slide. The electrodes were chlorinated before every use. The damp layer of filter paper beneath the enamel block must be in direct contact with the cell suspension. Excess liquid should be avoided to prevent movement of the coverslip and of the cell. The measuring electrodes were connected with a voltmeter and the input of an amplifier. The power electrodes were connected with the output of an amplifier. The current through the sample was regulated to keep the voltage drop across the measuring electrodes constant. The disadvantage of this galvanotaxis chamber is that products of electrolysis are not prevented from entering the chamber. Therefore, the measuring time must be kept short (<10 min). Longer measuring times can be achieved by periodically changing the polarity.

3. Collection and analysis of the data

The galvanotaxis chamber was placed on the heating stage of a phase contrast microscope (25 X). (The objective was kept on a constant temperature and had its own control unit). The temperature in the galvanotaxis chamber was calibrated (37 C) with a temperature-sensitive cholesteric liquid crystal as previously described (Ferguson 1968; Matthes and Gruler 1988).

The cell movement was observed with a video camera and recorded on VHS video tape (real time). The video signal was also digitized (Easytizer, Merlin Computer GmbH, Eschborn, FRG) for the computerized data analysis (Atari 1040 ST with hard disc. A flag in the digitizer was used to store the state of the applied voltage). Before this procedure the inhomogeneous illumination of the sample was eliminated by sending the video signal through a high pass filter ($f > 15$ kHz). A typical example of a digitized picture is shown in Fig. 1a.

The center of gravity of the cells is approximated by the center of area of the cell contour line. This procedure worked automatically very well as long as there was no cell-cell contact. The interval between consecutive images was 10 s, except in the E field-jump experiment (2 s). Typical trajectories of randomly and directed walking cells are shown in Fig. 1b and c. The trajectories were used to characterize the cellular responses as previously described (Rapp et al. 1988; Gruler 1989). The following mathematical procedures were applied, and we will describe them here in short.

Track velocity: The track velocity and its distribution function are important quantities for characterizing the chemokinetic response. The track velocity, v_c , is the ratio of the travelled distance, Δs , and the time difference, Δt . The track velocity distribution function was obtained by applying this procedure first along the path of one cell and then to all the other cells. All the measured values are sorted in a histogram. The normalized track velocity distribution density, $f(v_c)$, is obtained by dividing every column of the histogram by the total number of measured values and by the size of the segment, $2\pi v_c \cdot \Delta v_c$.

The track velocity autocorrelation function is an important procedure for the determination of signals which are hidden in the trajectories. The track velocity autocorrelation function $g_v(t_1 - t_2)$ was determined from the track velocity $v_c(t)$ of one cell as

$$g_v(t_1 - t_2) = \frac{\langle v_c(t_1) \cdot v_c(t_2) \rangle}{\sqrt{\langle v_c(t_1)^2 \rangle \cdot \langle v_c(t_2)^2 \rangle}} \quad (1)$$

Every average was performed over the time interval T . This procedure was repeated for many cells. The average is reported.

The track velocity autocorrelation function is constant if the track velocity is constant ($=v_{co}$). The temporal drop of the track velocity autocorrelation function is discussed thoroughly by Scharstein and Alt (1990).

Mean square displacement: The random walk activity can't be quantified by the mean displacement $\langle x(t) \rangle$ and

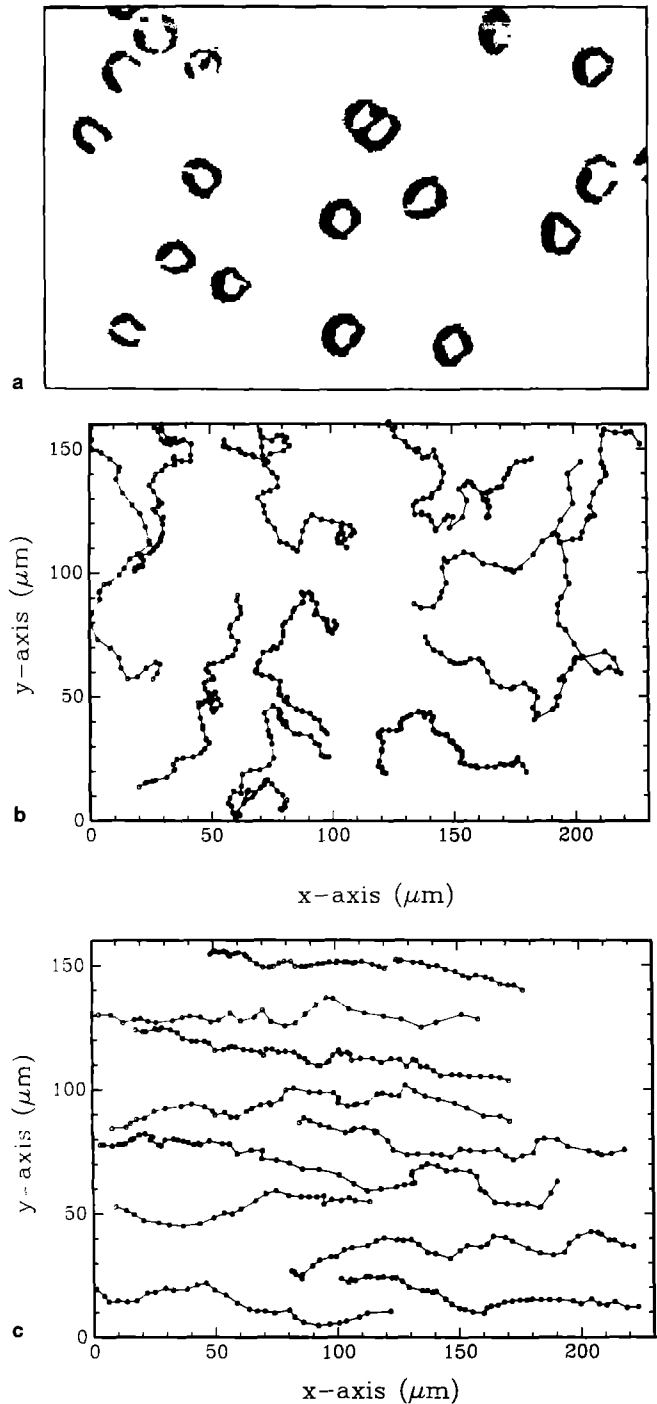


Fig. 1. a Digitized picture of migrating granulocytes (viewing field: $191 \cdot 129 \mu\text{m}^2$). b Trajectories of cells at random walk ($E = 0$ V/mm, $\langle \cos \Phi \rangle = 0.03 \pm 0.07$). c Trajectories of cells at galvanotaxis ($= 0.8$ V/mm, $\langle \cos \Phi \rangle = -0.87 \pm 0.01$)

$\langle y(t) \rangle$ since these quantities are zero owing to the symmetry of the cellular environment. However, the mean square displacements, $\langle x(t)^2 \rangle$ and $\langle y(t)^2 \rangle$, are non-zero values which can be used to quantify the random walk. A simplifying general tool is to assume a first-order fluctuation relaxation process or a directional jump process with exponential waiting times; the random walk process can then be described by the Langevin equation where the diffusion coefficient D and the characteristic

time τ are fitting parameters (Risken 1984; Haken 1983). Other models and formulas are given in "Biological motion" (Alt and Hoffmann 1990).

$$\langle x(t)^2 \rangle \quad \text{or} \quad \langle y(t)^2 \rangle = 2D \{t - \tau(1 - e^{-t/\tau})\} \quad (2)$$

It is important to note that the characteristic time involved in the random walk can be determined.

Polar order parameters: The directed movement can be quantified by the McCutcheon index. It is the mean drift velocity, $\langle v_{\parallel} \rangle$, divided by the mean track velocity, $\langle v_c \rangle$. The drift velocity is obtained by dividing the travelled distance, Δx , parallel to the applied electric field, by the time difference, Δt .

The directed movement can also be quantified by the average of $\cos \Phi$ where Φ is the angle between the direction of movement and the direction of the electric field.

The orientation autocorrelation function $g_P(t_1 - t_2)$ is an important procedure for looking for hidden signals in the trajectories. The orientation autocorrelation function $g_P(t_1 - t_2)$ was determined from the orientation angle $\Phi(t)$ of one cell as

$$g_P(t_1 - t_2) = \frac{\langle \cos \Phi(t_1) \cdot \cos \Phi(t_2) \rangle}{\sqrt{\langle \cos^2 \Phi(t_1) \rangle \cdot \langle \cos^2 \Phi(t_2) \rangle}} \quad (3)$$

Every average was performed over the time interval T . This procedure was repeated for many cells. The average is reported.

The orientation autocorrelation function can be interpreted in a similar way as the velocity autocorrelation function (Scharstein and Alt 1990).

Time-difference distribution function: The cellular relaxation or adaptation to a sudden jump in the physical environment yields information on the cellular transduction/response mechanism. The time difference between the change in the electric field and the change in moving direction can be determined from the trajectories. A change in moving direction is recognized if the turn angle averaged over several points is above an arbitrarily set clip level. The change in the cellular response can be determined for most cells. The change of moving direction at a constant electric field is hard to detect. But after switching the field from + to -, the rotation angles are large and therefore easier to recognize.

III. Results

1. Non-directed migration

The random movement of granulocytes was obtained when no voltage was applied. The mean displacements in the x and y direction and the average of $\cos \Phi$ should be zero if there is no gradient of any kind. Therefore, these quantities are used as control parameters for the chamber. For example the average of $\cos \Phi$ is 0.02 ± 0.07 in Fig. 1 b indicating no anisotropic environment.

The mean square displacement in the x and y direction can be used to quantify the random walk activity. A

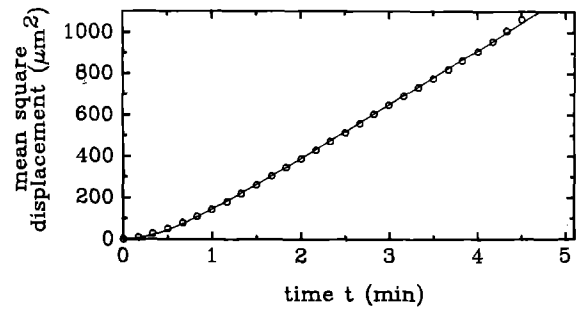


Fig. 2. Mean square displacement as a function of time. Dots obtained from 30 cells at 738 different starting positions. The line is a fit of (2) to the data ($D = 131.7 \mu\text{m}^2/\text{min}$, and $\tau = 32.1 \text{ s}$)

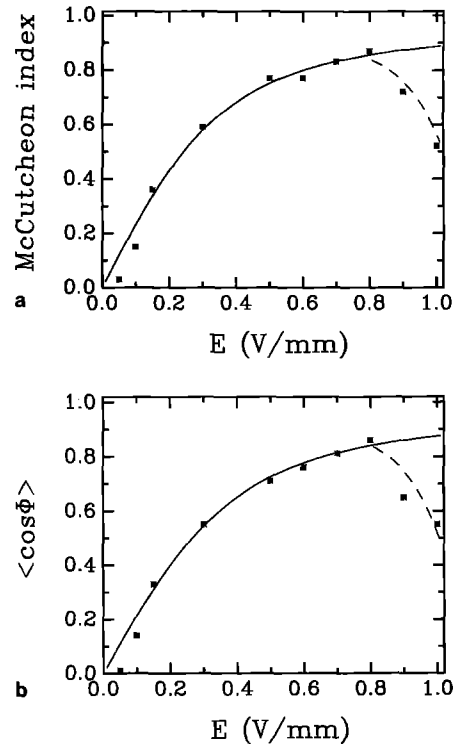


Fig. 3a, b. Galvanotactic dose-response curve. The dose is the mean applied electric field strength, E , and the cell response is in a the McCutcheon index and b the average of the cell orientation ($= \langle \cos \Phi \rangle$). The mean number of cells per data point is 34. It varies from 16 to 71. The line is a fit of (4) and (5) to the data. The dashed line is a fit of (4) and (6) to the data ($E > 0.78 \text{ V/mm}$). McCutcheon index data ($K_G^{-1} = -0.21 \text{ V/mm}$, $K_I = 3.2$) and $\langle \cos \Phi \rangle$ -data ($K_G^{-1} = -0.23 \text{ V/mm}$, $K_I = 3.7$)

typical result is shown in Fig. 2. The points were obtained from trajectories of 30 cells (738 different starting positions were chosen for the procedure). The Langevin equation (2) is fitted to the data. The fitting parameters are the diffusion coefficient D ($= 131.7 \pm 1.5 \mu\text{m}^2 \cdot \text{min}^{-1}$) and the characteristic time τ ($= 32.1 \pm 0.9 \text{ s}$) involved in random walk.

2. Directed migration

The random movement became directed, when an electric field was applied. The cells drift with a mean drift veloc-

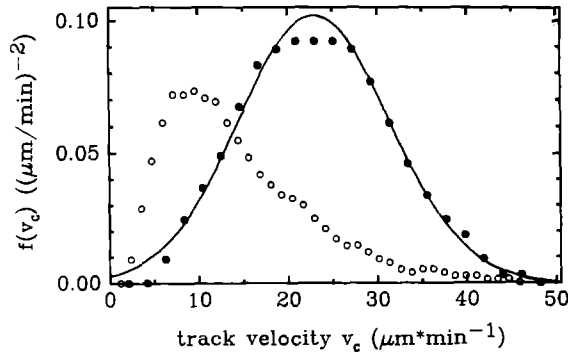


Fig. 4. Track velocity density distribution $f(v_c)$. 0.2 V/mm (open circle, a preparation with a bad galvanotactic response) and 0.6 V/mm (closed circle, a preparation with a good galvanotactic response). The line is a fitted gaussian curve ($v_c^{\text{det}} = 23 \mu\text{m}/\text{min}$ and $\sigma = 8.5 \mu\text{m}/\text{min}$)

ity, $\langle v_{\parallel} \rangle$, towards the anode. The McCutcheon index, $\langle v_{\parallel} \rangle / \langle v_c \rangle$, and the average of $\cos \Phi$ were used to quantify the directed movement. Both parameters increased monotonically with increasing field strength as long as $E < 0.78 \text{ V/mm}$. Above 0.78 V/mm both parameters decreased with increasing field strength as shown in Fig. 3 a and b.

The measured galvanotactic dose-response curve can be compared with a theoretical prediction (Gruler and Nuccitelli 1986; Gruler 1988; Gruler 1990).

$$\langle \cos \Phi \rangle = \frac{I_1(a_1)}{I_0(a_1)} \quad (4)$$

$$a_1 = K_G \cdot E \quad \text{for } E < E_0 = 0.78 \text{ V/mm} \quad (5)$$

$$a_1 = K_G \cdot (E - K_I(E - E_0)) \quad \text{for } E > E_0 = 0.78 \text{ V/mm} \quad (6)$$

I_1 and I_0 are hyperbolic Bessel functions. In the case of no inhibition the only fitting parameter is the galvanotaxis coefficient, K_G . We found $(-0.21 \text{ V/mm})^{-1}$ and $(-0.23 \text{ V/mm})^{-1}$ for the McCutcheon index and $\langle \cos \Phi \rangle$, respectively, as compared to $(-0.17 \text{ V/mm})^{-1}$ and $(-0.22 \text{ V/mm})^{-1}$ reported by Rapp et al. (1988). The inhibition coefficient above E_0 was 3.2 (McCutcheon index) and 3.7 ($\langle \cos \Phi \rangle$).

An important observation was, that the error bars of the polar order parameters and the chemokinetic activity of the cells are correlated. The error bars (=SDM) are, of course, a function of the number of cells. But besides this statistical error there is also a systematic error involved. The investigation of the chemokinetic response showed, that cells which had a good chemokinetic response had a good directed response, too. The track velocity density distribution, $f(v_c)$, was a gaussian (line fitted to the full circles in Fig. 4) yielding a good galvanotactic response with a small error in the polar order parameters. In the case of a diminished galvanotactic response and a relatively large error in the polar order parameters, the track velocity distribution density exhibited systematic deviations from the gaussian curve (open circles in Fig. 4). The track velocity distribution density can be described by two gaussian distributions. Only those cells with a good chemokinetic response were used in Fig. 3 a and b.

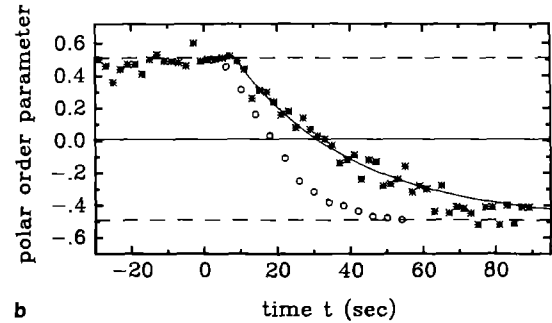
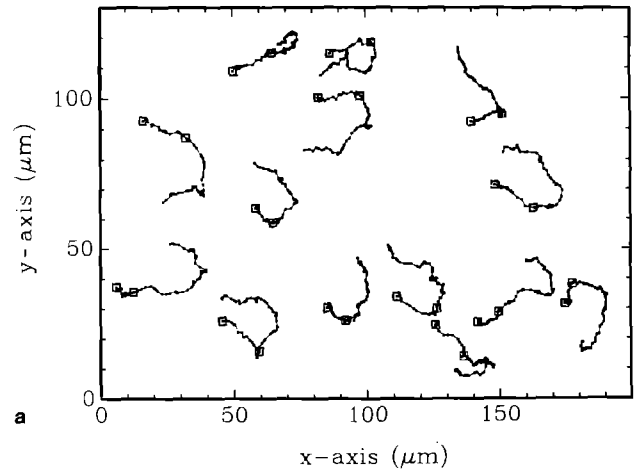


Fig. 5a, b. E-jump measurement with an electric field of 1 V/mm (98 cells). **a** Trajectories with $\Delta t = 2 \text{ s}$. The squares indicate the starting position and the position where the electric field was changed. **b** $\langle \cos \Phi \rangle$ as a function of time (*). The electric field changed sign at $t = 0$. The dashed lines indicate the two steady state values. The line is an exponential decay function with a characteristic time of 32.4 s. The open circles are derived from the time-difference-distribution function ((22) and (23))

An important ion in the cellular response is Ca^{++} and therefore it is of basic interest to understand the signal transduction/response mechanism. The galvanotactic response in serum (2.5 mM Ca^{++}) was always negative (in opposite direction to the applied electric field vector – towards the anode). However, in serum-free medium containing 0.1 mM Ca^{++} , the galvanotactic response was positive (in the direction of the applied electric field vector – towards the cathode) (McCutcheon index $+0.31 \pm 0.14$ and $\langle \cos \Phi \rangle +0.31 \pm 0.09$ (15 cells) at 1 V/mm). The control (2.5 mM Ca^{++}) exhibited a negative galvanotactic response (towards the anode) (McCutcheon index -0.18 ± 0.09 and $\langle \cos \Phi \rangle -0.15 \pm 0.07$ (29 cells).

3. E-jump and galvanotactic relaxation or adaptation process

The dynamic behaviour of the cellular signal transduction/response mechanism can be determined if the extracellular signal is varied in time. The electric field as the extracellular signal is the most suitable candidate for this type of experiment since the signal is fast and easy to apply to many cells simultaneously.

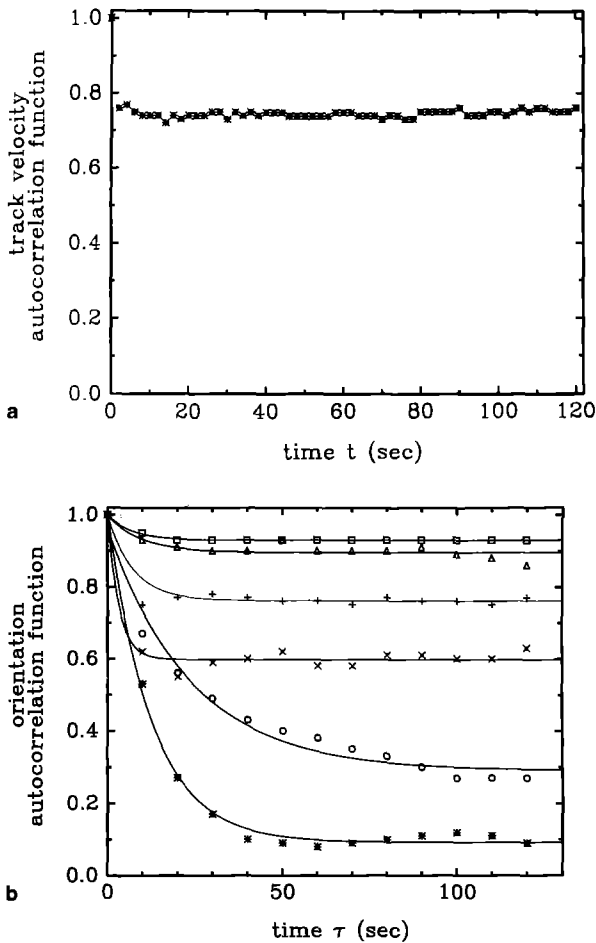


Fig. 6. **a** Track velocity autocorrelation function (48 cells and 1281 starting positions). **b** Orientation autocorrelation function (typical values: 15 to 30 cells, and 300 to 1300 starting positions). 5 field strength where the cells have a linear response: 0 V/mm (*), 0.15 V/mm (o), (+) 0.5 V/mm, (Δ) 0.6 V/mm, (\square) 0.8 V/mm, and 1 field strength where the cells have an inhibited response: (\times) 0.9 V/mm. Exponential decay functions are fitted to the data. The saturation value and the characteristic time are shown in Fig. 7a and b

First, the electric field was applied for approximately 3 min to equilibrate the cells to their environment. In the last two minutes before the electric field was altered from $-E$ ($t < 0$) to $+E$ ($t > 0$), the mean galvanotactic response was determined as $\langle \cos \Phi \rangle_{-E}$. The cellular response would be a step function as the electric field if the cells could react immediately ($\langle \cos \Phi \rangle_{-E}$ for $t < 0$ and $\langle \cos \Phi \rangle_{+E}$ for $t > 0$ with $|\langle \cos \Phi \rangle_{-E}| = |\langle \cos \Phi \rangle_{+E}|$). However, the cells required some time to react to the new environmental condition as shown in Fig. 5a. Two features were remarkable. (i) There existed a lag-time. The cells showed their first reaction to the changed environment after 8.3 s. (ii) The adaptation or relaxation process can be described by a single exponential function with a characteristic time of 32.4 ± 2.3 s (Fig. 5b).

4. Track velocity autocorrelation function

The track velocity autocorrelation function led to the following results (Fig. 6a): (i) The autocorrelation func-

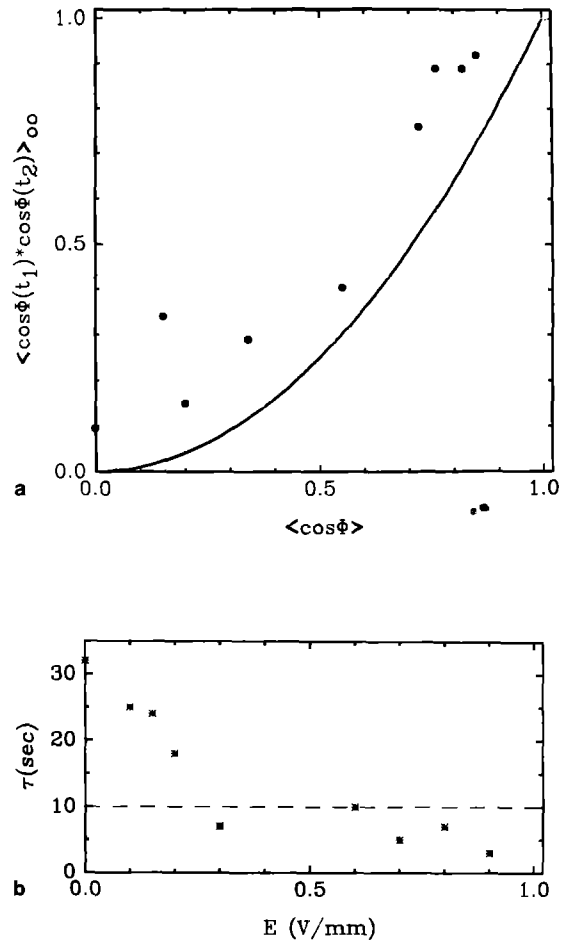


Fig. 7. **a** The saturation value of the orientation autocorrelation function as a function of $\langle \cos \Phi \rangle$. The dots are obtained from Fig. 6b (not all measurements are shown in Fig. 6b). The line is a theoretical prediction. **b** The characteristic time as a function of electric field strength. The dots are obtained from Fig. 6b. The time interval, Δt , of the measurement is a lower limit of the characteristic length (dashed line). The points below the dashed line show a tendency to small characteristic times with increasing field strength

tion decreased from 1.0 to 0.75 within 2 s. (ii) The track velocity autocorrelation function is a horizontal line after 2 s. The track velocity did not show the characteristic time of random walk. (iii) The track velocity autocorrelation function is independent of the applied electric field.

5. Orientation autocorrelation function

The direction determined from the trajectories showed temporal variations. The following results were obtained (Fig. 6b): (i) The orientation autocorrelation function is a function of the applied electric field strength. (ii) At large electric field strength the orientation autocorrelation function decreases within 10 s from one to a constant saturation value of about 0.9. (iii) The orientation autocorrelation function decays exponentially in time to a low saturation value for low electric field strengths. The saturation value as a function of $\langle \cos \Phi \rangle$ is shown in Fig. 7a. (iv) The characteristic time as a function of the applied electric field strength is shown in Fig. 7b.

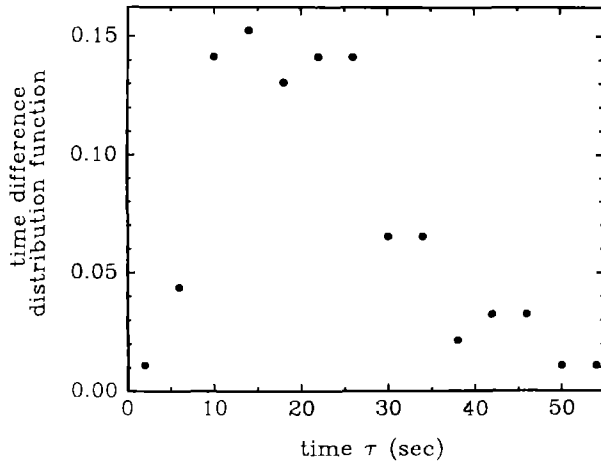


Fig. 8. Time difference distribution of E-jump experiment (1 V/mm)

6. Time-difference distribution function

The period between the change of electric field and of moving direction was investigated for 101 cells. For 9 cells it was not possible to decide when they changed their moving direction. The results are shown in a histogram (Fig. 8). Only a small fraction of the cells reacted in the first 8 s. The maximum was between 10 and 25 s. For a long period of time, the distribution decayed to zero.

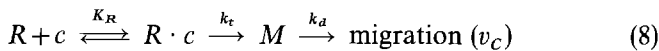
IV. Discussion

1. Chemokinetic response

We propose a model for the chemokinetic response adopted from Tranquillo and Lauffenburger 1987; Tranquillo et al. 1988 a) which is in analogy to enzyme kinetics. The basic assumptions are that a chemokinetic molecule (concentration $[c]$) binds reversibly to the membrane-bound receptor (equilibrium binding constant K_R) and that the track velocity is proportional to the second messenger, M . The total number of bound receptors is then regarded as the primary cellular signal, S ($= [R \cdot c]$).

$$S = R_0 \frac{[c]}{[c] + K_R} \quad (7)$$

R_0 is the total number of receptors per cell. This primary signal is amplified by biophysical and biochemical reactions to generate intracellular signals, M , which are considered here to be critical regulators of the motility system.



k_t represents the chemokinetic transduction rate constant and k_d^{-1} is the decay time of the intracellular signal. The rate equation for the intracellular signal is then

$$\frac{dM}{dt} = k_t \cdot S - k_d \cdot M + \Gamma(t) \quad (9)$$

where $\Gamma(t)$ is the noise in the signal transduction/response system. It is assumed that the chemokinetic response, v_c , is proportional to the concentration of the second messenger, M ($v_c = A \cdot M$).

The model leads to the stochastic differential Eq. (9). The model assumptions inherent in the stochastic differential Eq. (9) are that the migration steps stochastically change without any-time correlations but deterministically driven by the mean concentration. A deterministic value for the track velocity is obtained in the noise-free case. But with noise only the probability for the track velocity (within a certain segment) can be determined. We will show that the measured steady state chemokinetic dose-response curve as well as the measured track velocity distribution density are in accordance with the simple model.

The steady state chemokinetic dose-response curve obtained from (7) and (9) is determined by the equilibrium binding constant of the receptor. Thus the predicted dose-response curve has the same concentration dependence as the reversible binding process of chemokinetic molecules to the membrane-bound receptor. This predicted chemokinetic dose-response curve was found by several groups (Becker et al. 1978; Zigmond and Sullivan 1981; Wilkinson 1982; Gruler and Bültmann 1984; Gruler 1989).

The track velocity distribution function can be obtained from the Fokker-Planck equation which is derived from (9) (Haken 1983; Risken 1984; Gruler 1990). The solution is a gaussian if a white noise source (noise source strength q) is assumed.

$$f(M) = C e^{-1/q (-2 k_t \cdot S \cdot M + k_d \cdot M^2)} \quad (10)$$

C is a calibration constant. If it is assumed that the track velocity is proportional to the concentration of the second messenger then the second messenger distribution density, $f(M)$, equals the track velocity distribution density, $f(v_c)$. We showed that cells with a good galvanotactic response have a gaussian track velocity distribution density as predicted by the model. The single gaussian is evidence that the cells are a homogeneous population of cells where the chemokinetic response fluctuates around a mean response. In addition we showed previously (Gruler 1984) that the track velocity density of a single cell when the cell is observed over a long period of time, is identical with the track velocity density of many cells, when the cells were only observed over a small period of time. The maximum and the width of the gaussian are determined by the deterministic and stochastic signal in the second messenger, respectively. Consequently, the quality of a cell preparation can be quantified by measuring the track velocity distribution density, $f(v_c)$. The first criteria is whether $f(v_c)$ is a gaussian or not. Even if the density is a gaussian and the preparation is considered as good, there are further possibilities to distinguish between different preparations. The ratio of velocity at the maximum, v_c^{det} , and the width of the distribution, σ can be regarded as the signal-to-noise ratio of the chemokinetic response, S/N (see (9)).

The signal-to-noise ratio obtained from the distribution shown in Fig. 4 was 2.7. (The cell were exposed to 50% plasma and 50% HBSS). The signal-to-noise ratio

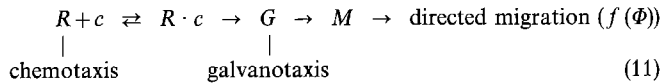
can increase to 3.8 if the granulocytes were exposed to 100% plasma (de Boisleury-Chevance et al. 1989; Gruler and de Boisleury-Chevance 1987). The signal-to-noise of a preparation of Ramsey (1972) was 1.5. We used the signal-to-noise ratio as a control parameter in our later experiments. It was always larger than 1.5.

We expect, that the basic noise source is at the initiation of the signal chain. Receptor binding fluctuations are assumed in the case of chemotaxis (Tranquillo and Lauffenburger 1987; Tranquillo et al. 1988a). This cannot be the case in chemokinesis because the track velocity autocorrelation function is a horizontal line. Therefore the noise signal must be a slow varying function. The track velocity must vary in time, otherwise the distribution density of the single cell could not be identical with that obtained from many cells.

2. Galvanotactic response

Granulocytes have the ability to orient their movements along an applied electric field. The mean displacement of the cells is quantified by the mean velocity parallel to the applied electric field (= drift velocity) times the observation time. The drift velocity is the product of the mean track velocity times the average of $\cos \Phi$ since the McCutcheon index equals $\langle \cos \Phi \rangle$ (Fig. 3a and b; Gruler 1984; Rapp et al. 1988). This means that the temporal variations in the track velocity are uncorrelated with the temporal variations of direction of migration. This puzzling result is now understandable since the track velocity is a constant (within a few minutes).

The galvanotactic response is quantified by an angle distribution density, $f(\Phi)$, which is a bell-shaped curve with its maximum towards the anode. The aim is to derive the galvanotactic distribution density, $f(\Phi)$, as in the case of chemokinesis from a simple model. The early events in the chemokinetic and the chemotactic response are: The loaded chemokinetic (or chemotactic) receptor stimulates the *G*-protein and it stimulates in turn further proteins resulting in the migration (Becker et al. 1987). The *G*-protein is the likely essential protein in galvanotaxis since the *G*-protein and the galvanotactic response have the same isoelectric point of 5.7 (Rapp et al. 1988).



The number of occupied membrane-bound receptors is considered as the primary signal in chemokinesis. In chemotaxis, it is assumed that the cell measures the concentration of chemotactic molecules at two separate parts of the membrane. For simplicity only two parts located perpendicular to the direction of migration, are considered. The difference of the number of the occupied receptors at the two membrane patches is then considered as the primary signal (Gruler 1988, 1990).

$$\begin{aligned} \Delta S(\Phi) &= [R \cdot c]_L - [R \cdot c]_R \\ &= \frac{R_0}{2} \cdot \frac{K_R}{([c] + K_R)^2} \cdot \frac{d[c]}{dx} \cdot l_0 \cdot \sin \Phi \end{aligned} \quad (12)$$

l_0 is the distance between the two membrane patches. This primary cellular signal is the cause for a change of direction of migration. The stochastic differential equation for the direction of migration is then

$$\frac{d\Phi}{dt} = -k_t \cdot \Delta S(\Phi) + \Gamma(t) \quad (13)$$

where k_t is a chemotactic signal transduction constant. The first term on the right side is the deterministic signal which can be understood as a virtual torque acting on the cell. The second term is a stochastic function. If a white noise source is assumed as in the chemokinetic model, then the steady state angle distribution function is (Haken 1983; Risken 1984; Gruler 1990) (C is a calibration constant).

$$f(\Phi) = C \cdot e^{a_1 \cos \Phi} \quad (14)$$

$$a_1 = k_t \cdot l_0 \cdot \frac{R_0}{q} \cdot \frac{K_R}{([c] + K_R)^2} \cdot \frac{d[c]}{dx} \quad (15)$$

The simple model predicts an angle distribution density as actually measured and the measured concentration dependence of a_1 is in accordance with the model (Gruler 1988; Tranquillo et al. 1988b; Gruler 1990). Obviously, the hypothesis of a spatial recognition system for measuring the concentration gradient is consistent with the recorded data.

Galvanotaxis can also be described by a spatial recognition system: The cell measures the potential difference at two separated parts of the membrane and the primary cellular signal would be the concentration difference of charged membrane-bound *G*-protein. The rate equation for the direction of migration is

$$\frac{d\Phi}{dt} = -k_t \cdot \frac{R_0}{2} \cdot l_0 \cdot E \cdot \sin \Phi + \Gamma(t) \quad (16)$$

The cells drift parallel to the applied electric field if the galvanotactic transduction rate coefficient, k_t , is positive and they drift antiparallel if k_t is negative. The steady state angle distribution density, $f(\Phi)$, is again described by (14) with

$$a_1 = k_t \cdot \frac{R_0}{q} \cdot l_0 \cdot E \quad (17)$$

If there were no noise in the signal chain, then the cells would migrate parallel to the applied polar field and the distribution $f(\Phi)$ would be a δ -function. The width of $f(\Phi)$ is as expected proportional to the noise source strength. In chemotaxis (Tranquillo and Lauffenburger 1987; Tranquillo et al. 1988a) the receptor binding fluctuations are discussed as a likely noise source, in galvanotaxis the fluctuations of the *G*-protein density can be considered as a likely noise source.

The model assumptions inherent in the stochastic differential Eqs. (13) (galvanotaxis) and (16) (chemotaxis) are that the migration angle stochastically changes without any time correlations or external directional bias, but is deterministically driven towards the orientation field

angle. Thus, the directional response mechanism itself would not be of stochastic nature.

The applied electric field, E , can create (i) an electric field parallel to the surface of the membrane as well as (ii) a change in the membrane potential difference across the cell membrane. The first mechanism is considered as the origin of the linear response where charged membrane-bound particles are distributed by lateral electrophoresis. This linear response holds as long as the applied electric field strength is less than 0.78 V/mm. But at high field strength the second mechanism also becomes important and we expect some deviation from the linear response. The potential difference of the membrane facing the anode, is hyperpolarized by the applied electric field ($\Delta V = -17.5$ mV for a 15 μm spherical cell and for a field strength of 0.78 V/mm). The membrane potential difference, U , without an applied electric field is reported as -34.4 ± 24 mV (Jäger et al. 1988), -53 mV or -67 mV (Gallin and McKinney 1989). The K^+ ion is likely to be responsible for the inhibition since the approximate equilibrium potential for Na^+ , K^+ , Cl^- , and Ca^{++} ions are $+46$, -95 , -7 , and $+150$ mV, respectively (Gallin and McKinney 1989). These numbers show that the flux of potassium ions is very low or has reversed its direction at high electric field strengths. We expect that this second mechanism has an influence on the transduction rate coefficient, k_t . The inhibition is not unique for granulocytes. It is observed as well in the galvanotaxis of neural crest cells (Gruler and Nuccitelli, to be published) and in the galvanotropism of growing germ tubes and hyphae (McGillivray and Gow 1986; Gruler and Gow 1990). The inhibition can be so powerful that the response reverses as Van Laere (1988) has shown. Germ tubes and hyphae of *Phycomyces blakesleeanus* grew towards the anode at low field strength (<0.5 V/mm) and towards the cathode at high field strength.

We measured the galvanotactic response of granulocytes as a function of Ca^{++} concentration and found that there exists a critical concentration, c_0 . One could speculate, that the electrochemical potential is zero at this concentration so that there is no driving force for the ions. But this argument cannot be true since the low intracellular Ca^{++} concentration (0.1 μM for non-stimulated cells and 0.5–1.0 μM for stimulated cells (Hallett 1989)) and the negative potential in the cell forces the Ca^{++} ions to move into the cell. Therefore the sign change in the galvanotactic response cannot be induced by the Ca^{++} current. There must be another function of the Ca^{++} . Ca^{++} ions have many other ways to interact in the galvanotaxis signal chain, e.g. a Ca^{++} can induce conformational changes of an essential protein in the galvanotactic signal chain. The Ca^{++} -activation of the protein kinase C and of the phospholipase A_2 are discussed (Naccache et al. 1989). Other key Ca^{++} -binding proteins cannot, however, be excluded. The possibility also exists that some intracellular messengers act in complete independence of intracellular Ca^{++} (Cooke et al. 1989).

The temporal behaviour of the galvanotactic response can be investigated by inspecting the orientation autocorrelation function. Solving the stochastic differential

equation for small angle yields

$$\langle \Phi(t_1) \cdot \Phi(t_2) \rangle = A \cdot e^{-\frac{|t_1-t_2|}{\tau}} \quad (18)$$

$$\frac{1}{\tau} = \frac{1}{2} k_t R_0 l_0 E \quad (19)$$

$$A = \frac{q}{2} \cdot \tau \quad (20)$$

Two features are described by these equations. The characteristic time involved in galvanotaxis decreases with increasing field strength and the fluctuations in the direction of migration decrease with increasing field strength. But the prediction failed for random walk ($E=0$) where the characteristic time approaches infinity.

The orientation autocorrelation function, $\langle \cos \Phi(t_1) \cdot \cos \Phi(t_2) \rangle$, has at least three contributions

$$\langle \cos \Phi(t_1) \cdot \cos \Phi(t_2) \rangle = B \cdot \delta(t_1 - t_2) + \frac{q\tau}{2} \cdot e^{-\frac{|t_1-t_2|}{\tau}} + \langle \cos \Phi \rangle^2 \quad (21)$$

Uncertainty in measurements of cell positions and fast random cellular processes are approximately summarized in the first term. This term describes the drop of the autocorrelation function for $t_1 \sim t_2$. The second term quantifies the characteristic time involved in migration. (It is assumed that the small angle solution (Eq. (21)) also holds for $\cos \Phi$). The third term describes the saturation value of the orientation autocorrelation function for $|t_1 - t_2| \rightarrow \infty$. For large $|t_1 - t_2|$ the temporal variations of $\cos \Phi(t_1)$ and of $\cos \Phi(t_2)$ are uncorrelated and hence $\langle \cos \Phi(t_1) \cdot \cos \Phi(t_2) \rangle_\infty$ is simply $\langle \cos \Phi \rangle^2$. The saturation value of the orientation autocorrelation function is shown as a function of $\langle \cos \Phi \rangle$ in Fig. 7a. The theory predicts a parabola. The measured values are systematic above the predicted values. The systematic deviation can be explained by a second exponential decay function with a large characteristic time but a small amplitude. This second characteristic time is more pronounced in the case of migrating monocytes (de Boisfleury-Chevance et al. 1989) and the mean square displacement as a function of time is never a straight line for long time intervals. The values of the second characteristic time constants are larger than 2 min (granulocytes) and 18 min (monocytes). It is difficult to determine the second characteristic constant with the described apparatus since the cells leave the viewing field too fast. A second and large characteristic time was also observed in contact guidance when granulocytes oriented their movement along grooves in the substrate (Matthes and Gruler 1988).

3. Galvanotaxis relaxation (or adaptation) process

The cell cannot react immediately to the altered signal since the chemistry and physics involved in the migration process needs some time to form new products and to rearrange the cellular structure. In the case of granulocytes at 37 C it is 8.3 s. A lag-time of several seconds is

expected since the cycle time of protein complexes as e.g. the monooxygenase P-450 have a cycle time of 1.5 s (Müller-Enoch et al. 1984). A lag time of about 10 s is visible directly in time lapse-movies showing the necrotactic response after lysing a red blood cell (Gruler 1984).

The relaxation (or adaptation) is explained by the measured time-difference distribution and an all-or-nothing model. For simplicity, let us assume that a cell which has registered the new field direction will show a mean response of $\langle \cos \Phi \rangle_{-E}$ and that the cells, which have not yet registered the altered field will have a mean response of $\langle \cos \Phi \rangle_{+E}$. The time-dependence of $\langle \cos \Phi \rangle$ is then

$$\langle \cos \Phi(t) \rangle = n_{\text{Reg}} \cdot \langle \cos \Phi \rangle_{+E} + n_{\text{Non}} \cdot \langle \cos \Phi \rangle_{-E} \quad (22)$$

The fraction of cells, which have registered the electric field, is calculated from the time-difference distribution function, $f(t)$, as

$$n_{\text{Reg}}(t) = \int_0^t f(t') dt' \quad (23)$$

The results is shown as dots in Fig. 5b. The discrepancy between the prediction and the measurements is due to the fact that the cells need some time for the reorientation. The time-difference distribution function measures only the beginning of the reorientation process.

The cells performed a large change in moving direction in the E-jump experiment. The measured characteristic time of this relaxation (or adaptation) phenomena was 32.4 s (Fig. 5a). A similar characteristic time of 32.1 s was measured in the case of random migration (Fig. 2). The E-jump experiment can be interpreted in the following way. When the electric field is altered, then the cells react very fast (characteristic time 32 s). After the characteristic time of 32 s the cells move approximately in the new direction and then the second (long) characteristic time is important. In this cellular mode the cell integrates the input signal over a long period of time. The merit of the long characteristic time constant is, that the noise in the signal transduction system is eliminated to a large extent. The disadvantage of a long characteristic time is that the system is inert to fast changes in moving direction.

4. Steerer and automatic control

The directed movement of granulocytes can be divided into two independent processes. One for the movement of the center of mass and another for the direction of migration. Hence, the track velocity and the angle of migration are two independent state variables. This fact was shown for chemotaxis (granulocytes, Bültmann and Gruler 1983), galvanotaxis (granulocytes, Rapp et al. 1988 and this paper; somitic fibroblasts, Gruler and Nuccitelli 1986; neural crest cells, Gruler and Nuccitelli, will be published), and necrotaxis (granulocytes, Gruler 1984; monocytes, de Boisleury et al. 1989). Two different cellular actions are expected to predict the values of the two independent state variables as a function of the exogenous signal. The model for the chemokinetic activity is a

steerer and for the angle of migration an *automatic controller*.

The *steerer* is a controller without feedback. The hallmarks of a steerer are first an element which *measures* the environment and second a means for feeding an *output* which is proportional to the input signal. In a steerer there is no means for controlling the output. Here, the cell has a device for measuring the mean concentration of chemokinetic molecules. The received signal governs the apparatus of motility. The cell does not control whether the actual speed is smaller or larger than the expected one (no feedback loop). The steerer as a model for the chemokinesis is based on the observation that the mean speed is proportional to the mean concentration of membrane-bound receptors loaded with chemokinetic molecules. Hence, the stochastic differential Eq. (9) which is experimentally verified, holds also for a steerer device (Gruler 1990).

An important concept in understanding biological phenomena is cybernetics, also known as the theory of the *automatic control* (Wiener 1961). The theory of automatic controls is widely used in physiology and neurophysiology. It is shown that chemotaxis, galvanotaxis, galvanotropism, etc. are functions of cells having an automatic controller as goal-seeking system (Gruler 1990; Gruler and Franke, to be published).

We have the following situation: A cell is exposed to a vector field and the cell tries to follow the field lines. The migration is the output of the cell. The output is regulated by means of the input signal. This is a typical situation of a device with an automatic control. The hallmarks of automatic control are first an element which *measures* the output; second, a means of *comparing* that output with the desired output; third, a means of *feeding back* this information to the input in a way that minimizes the deviation of the output from the desired level. There exist several types of automatic control and here we are interested in which type of automatic control the cell is using.

Proportional controller: The hypothesis is that the cell determines its orientation in respect to the vector field by measuring the signal at two separate membrane-patches. The cell is positioned in the desired orientation when the two signals are equal. The advantage of the proportional control is that a cell can react fast to an altered environment while its disadvantage is that only a finite number of receptors or G-proteins are involved and hence the cell cannot measure its angle very accurately.

The temporal change of the migration angle has two sources: (i) a deterministic source which is fed by the ideal signal difference and (ii) a stochastic source which originates from the noise in the system. The stochastic differential equation of the proportional controller is identical with the discussed stochastic differential Eqs. (13) and (16) and hence, the hypothesis of the proportional controller as goal-seeking system is consistent with the recorded data. But at low polar field strength where the signal difference is low, deviations from the proportional controller are observed (Gruler 1990; Gruler and Franke, to be published).

Integral controller: The hypothesis is that the cell integrates its orientation over time. The temporal change of direction of migration is proportional to the orientation integrated over a time interval. The positive feature of such a controller is that the desired output can be very accurately approached since integration reduces the stochastic fluctuations. The negative features are (i) the controller is slow and (ii) an integral controller alone is unstable – it is an oscillator.

Proportional integral controller: The hypothesis that the cell acts like a proportional-integral controller, is consistent with the recorded data even at low field strength (Gruler 1990; Gruler and Franke, to be published). The model predicts an oscillatory state at low or no field strength which could partially explain the random walk. At high field strength the component of the proportional controller is dominant.

The Tranquillo-Lauffenburger chemotaxis model (Tranquillo and Lauffenburger 1987; Tranquillo et al. 1988a; Tranquillo 1990) is closely related to a proportional-integral controller but unfortunately they have not recognized the feedback loop in the signal transduction/response system. They assumed in detail: (i) The input signal for the directional movement is a spatial difference in receptor-measured concentrations. (ii) The receptor signal is transformed in an internal signal (second messenger). (iii) The cell turning rate is proportional to the difference in receptor signals. These features (i to iii) actually describe a proportional steerer but they are also necessary for a proportional controller. (iv) The receptor binding fluctuates in time and is thus the noise source in the system. We assumed a white noise without knowing the origin of the source. (v) The cell has some means (as we assumed) by which it can time-average the fraction of bound receptors so as to reduce the noise in the associated receptor-measured concentration (= integral controller). Tranquillo et al. concentrated their efforts on various aspects such as receptor binding, second messenger, etc. connected with cellular turning behaviour. Consequently, the Tranquillo-Lauffenburger chemotaxis model can make predictions on such subjects. But if only the phenomenon of the directed movement is of interest the automatic controller is the more appropriate model.

The theory of the automatic control is an important concept in understanding biological phenomena. This study wants to place the directed phenomena such as chemotaxis, galvanotaxis, directed growth, etc. in a better perspective. The phenomenological description of biological systems by its control units allows the modelling of biological systems even when a detailed knowledge is missing. Other biological phenomena where feedback and control are essential, can be investigated in a similar way.

Acknowledgement. This work was supported by "Fond der chemischen Industrie" and by a NATO travel grant.

References

- Alt W, Hoffmann G (eds) (1990) Biological motion. Springer, Berlin Heidelberg New York
- Becker EL, Showell HJ, Naccache PH, Sha'afi R (1978) Enzymes in granulocytes movement: preliminary evidence for the involvement of Na^+ and K^+ ATPase. In: Gallin JI, Quie PG (eds) Leukocyte chemotaxis. Raven Press, New York, pp 113–121
- Becker EL, Kanaho Y, Kermode JC (1987) Nature and functioning of the pertussis toxin-sensitive G-protein of neutrophils. *Biomed Pharmacol* 41:289–297
- de Boisleury-Chevance A, Rapp B, Gruler H (1989). Locomotion of white blood cells: a biophysical analysis. *Blood Cells* 15:315–333
- Cooke E, Al-Mohanna FA, Hallett MB (1989) Calcium-dependent and independent mechanisms of cellular control within neutrophils: the roles of kinase C, diacylglycerol, and unidentified intracellular messengers. In: Hallett MB (ed) The neutrophil: cellular biochemistry and physiology. CRC Press, Boca Raton, pp 219–241
- Erickson CA, Nuccitelli R (1984) Embryonic fibroblast motility and orientation can be influenced by physiological electric fields. *J Cell Biol* 98:296–307
- Ferguson JL (1968) Liquid crystals in nondestructive testing. *Appl Opt* 7:1729–1737
- Fukushima K, Senda N, Innui H, Tamai Y, Murakami Y (1953) Studies of galvanotaxis of leukocytes. *Med J Osaka Univ* 4:195–208
- Fukushima K, Senda N, Ishigami S, Murakami Y, Nishian K (1954) Dynamic pattern in the movement of leukocyte II. The behaviour of neutrophil immediately after commencement and removal of stimulation. *Med J Osaka Univ* 5:47–56
- Gallin EK, McKinney LC (1989) Ion transport in phagocytes. In: Hallett MB (ed) The neutrophil: cellular biochemistry and physiology. CRC Press, Boca Raton, pp 243–259
- Gerish G, Keller H-H (1981) Chemotactic reorientation of granulocytes stimulated with micropipettes containing f-Met-Leu-Phe. *J Cell Sci* 52:1–10
- Gruler H (1984) Cell movement analysis in a necrotactic assay. *Blood Cells* 10:107–121
- Gruler H (1988) Cell movement and symmetry of the cellular environment. *Z Naturforsch* 43c:754–764
- Gruler H (1989) Biophysics of leukocytes: neutrophil chemotaxis, characteristics and mechanisms. In: Hallett MB (ed) The cellular biochemistry and physiology of neutrophil. CRC Press, Boca Raton, pp 63–95
- Gruler H (1990) Chemokinesis, chemotaxis and galvanotaxis. In: Alt W, Hoffmann G (eds) Lecture notes in biomathematics. Springer, Berlin Heidelberg New York
- Gruler H, de Boisleury-Chevance A (1987) Chemokinesis and necrotaxis of human granulocytes: the important cellular organelles. *Z Naturforsch* 42c:1126–1134
- Gruler H, Bültmann BD (1984) Virus-induced order-disorder transition of moving human leukocytes. *Il Nuovo Cimento* 3D:152–173
- Gruler H, Franke K (1990) Automatic control and directed cell movement: (to be published)
- Gruler H, Gow NAR (1990) Directed growth of fungal hyphae in an electric field. A biophysical analysis. *Z Naturforsch* 45c:306–313
- Gruler H, Nuccitelli R (1986) New insights into galvanotaxis and other directed cell movements: an analysis of the translocation distribution function. In: Nuccitelli R (ed) Ionic currents in development. Liss, New York, pp 337–347
- Haken H (1983) Synergetics. Springer, Berlin Heidelberg New York, pp 146–189
- Hallett MB (1989) The significance of stimulus-response coupling in the neutrophil for physiology and pathology. In: Hallett MB (ed) The neutrophil: Cellular biochemistry and physiology. CRC Press, Boca Raton, pp 1–22

- Jäger U, Gruler H, Bültmann BD (1988) Morphological changes and membrane potential of human granulocytes under influence of chemotactic peptide and/or echo-virus, type 9. *Klin Wochenschr* 66:434–436
- Matthes T, Gruler H (1988) Analysis of cell locomotion. Contact guidance of human polymorphonuclear leukocytes. *Eur Biophys J* 15:343–357
- McGillivray AM, Gow NAR (1986) Applied electric fields polarize the growth of mycelial fungi. *J Gen Microbiol* 132:2515–2525
- Müller-Enoch D, Churchill P, Fleischer S, Guengerich FP (1984) Interaction of liver microsomal cytochrome P-450 and NADPH-cytochrome P-450 reductase in the presence and absence of lipid. *J Biol Chem* 259:8174–8182
- Naccache PH, Sha'afi RI, Borgeat P (1989) Mobilization, metabolism, and biological effects of eicosanoids in polymorphonuclear leukocytes. In: Hallett MB (ed) *The neutrophil: cellular biochemistry and physiology*. CRC Press, Boca Raton, pp 113–139
- Ramsey WS (1972) Analysis of individual leucocyte behavior during chemotaxis. *Exp Cell Res* 70:129–139
- Rapp B, de Boisfleury-Chevance A, Gruler H (1988) Galvanotaxis of human granulocytes. Dose-response curve. *Eur Biophys J* 16:313–319
- Risken H (1984) *The Fokker-Planck equation*. Springer, Berlin Heidelberg New York
- Scharstein H, Alt W (1990) Discretization problems. In: Alt W, Hoffmann G (eds) *Biological motion*. Springer, Berlin Heidelberg New York
- Tranquillo RT (1990) Models of chemical gradient sensing cells. In: Alt W, Hoffmann G (eds) *Biological motion*. Springer, Berlin Heidelberg New York
- Tranquillo RT, Lauffenburger DA (1987) Stochastic model of leukocyte chemosensory movement. *J Math Biol* 25:229–262
- Tranquillo RT, Lauffenburger DA, Zigmond SH (1988 a) A stochastic model for leukocyte random motility and chemotaxis based on receptor binding fluctuations. *J Cell Biol* 106:303–309
- Tranquillo RT, Zigmond SH, Lauffenburger DA (1988 b) Measurement of the chemotaxis coefficient for human neutrophils in the under-agarose migration assay. *Cell Motil Cytoskeleton* 11:1–15
- Van Laere AJ (1988) Effect of electrical fields on polar growth of *Phycomyces blakesleeanus*. *FEMS Microbiol Lett* 49:111–116
- Wiener N (1961) *Cybernetics: or control and communication in the animal and the machine*. MIT Press, Cambridge
- Wilkinson PC (1982) *Chemotaxis and inflammation*. Churchill Livingstone, Edinburgh London Melbourne
- Zigmond SH, Sullivan SJ (1981) Receptor modulation and its consequences for the response to chemotactic peptides. In: Lackie JM, Wilkinson PC (eds) *Biology of chemotactic response*. University Press, Cambridge London, pp 73–88